AN IMPROVED SPEED CONTROLLER FOR PMSM DRIVE WITH UNBALANCED LOAD USING LOAD TORQUE OBSERVER

A Thesis

by

Koray Yoldaş

Submitted to the
Graduate School of Sciences and Engineering
In Partial Fulfillment of the Requirements for
the Degree of

Master of Science

in the
Department of Electrical and Electronics Engineering

Özyeğin University
June 2019

AN IMPROVED SPEED CONTROLLER FOR PMSM DRIVE WITH UNBALANCED LOAD USING LOAD TORQUE OBSERVER

Approved by:

Assistant Professor Ahmet Tekin, Advisor
Department of Electrical and Electronics Engineering
Özyeğin University

Assistant Professor Göktürk Poyrazoğlu
Department of Electrical and Electronics Engineering
Özyeğin University

Assistant Professor Özkan Akın
Department of Electrical and Electronics Engineering
Ege University

Date Approved: 22 May 2019

ABSTRACT

In order to overcome disturbance effects as load torque variations in Permanent Magnet Synchronous Motor (PMSM), an improved controller with feed forward compensation is presented in this study. Washing machines which are a good application area of both variable loads and low-high speed operations is chosen to examine the effectiveness of the proposed method. Firstly, a mathematical model of permanent magnet synchronous motor and torque expressions of washing machine is reviewed. The Field Oriented Control is introduced with the Clarke and Park Transformations. Implementing the Field Oriented Control algorithm requires motor speed and rotor position information. In order to obtain these parameters, sensorless observer approach is used. Then for using in feedforward compensation of PMSM control system, load torque observer techniques have been studied. The observed torque is used as feedforward in q axis current PI controller to compensate the output of speed PI controller caused by unbalanced load profile of the washing machine. Motor speed information is required in both sensorless motor control alghorithm and in proposed feedforward compensation with load torque observer. In order to get best improvement by compensation, Extended Luenberger Observer, Direct Integration and Sliding Mode Observer methods are introduced with improvements for obtaining the motor speed. Simulation and experimental results are showed that in an operating system with disturbances as washing machines, PI controller response time can be improved by adopting an accurate feedforward scheme. Thus, energy efficiency performance, acoustical noise level and vibration performance of the washing machine can be improved by this method.

ÖZETÇE

Bu çalışmada çamaşır makinelerinin Sabit Mıknatıslı Senkron Motor (SMSM)'larında değişken yük torkları gibi bozucu etkilerin önüne geçilmesi için ileribeslemeli komponzasyon metodu içeren geliştirilmiş bir motor kontrolör sunulmuştur. Çamaşır Makineleri hem değişken yüklerin hem de düşük-yüksek hız profillerinin olması sebebiyle önerilen metodun etkisinin inceleneceği uygulama alanı olarak seçilmiştir. İlk olarak sabit mıknatıslı senkron motorun matematiksel modeli ve çamaşır makinesinin tork denklemleri çalışılmıştır. Daha sonra clarke ve park dönüşümleriyle vektör kontrolü uygulanmıştır. Vektör kontrol algoritması motor hızı ve rotor pozisyon bilgisini gerektirmektedir. Bu parametrelerin elde edilmesinde sensörsüz gözlemleyici yöntemi tercih edilmiştir. SMSM kontrol sisteminin ileribeslemeli komponzasyonunda kullanılması için yük torku gözlemleyici teknikleri çalışılmıştır. Çamaşır makinelerinde dengesiz yük profilinden gelen etkilerin kompanzasyonunda hız PI kontrolünden gelen kontrol parametresinin kompanzasyonu için gözlemciden elde edilen yük torku bilgisi q ekseni PI kontrolüne ileribesleme olarak eklenmiştir. Motor hızı bilgisi hem sensörsüz motor kontrol algoritmasında hem de önerilen yük torku gözlemleyicili ileribesleme kompanzasyonunda gerekmektedir. Motor hız bilgisini elde etmek için ve kompanzasyon ile en iyi gelişmeyi sağlamak için Genişletilmiş Luenberger Gözlemleyicisi, Doğrudan İntegrasyon ve Kayma Kipli Gözlemleyici yöntemleri sunulmuştur. Simülasyon ve deneysel çalışmaların sonucuna göre bozucu etkilerle çalışan çamaşır makineleri gibi uygulama alanlarında uygun bir ileribesleme kompanzasyon metodu kullanılarak PI kontrolörün tepki zamanı iyileştirilebilir. Bu sayede çamaşır makinelerinin enerji verimliliği performansı, akustik gürültü seviyesi ve titreşim performansı iyileştirilebilir.

ACKNOWLEDGEMENTS

First of all, I would like to thank my advisor Asst.Prof. Ahmet Tekin for his continuous guidance and support. I am also greatly indebted to Assoc. Prof. Mutlu Boztepe for offering his guidance through the various technical challenges encountered in completing this thesis.

I am also thankful to my company VESTEL for all opportunities. I would also like to acknowledge Mr. Serkan Balcı of the R&D Manager at the VESTEL Washing Machine Plant for encouraging me in every step of this study.

Finally, I must express my very profound gratitude to my family for providing me with unfailing support and continuous encouragement throughout my years of study.

TABLE OF CONTENTS

LIST OF TABLES

LIST OF FIGURES

LIST OF SYMBOLS

β_q Field weakening coefficient

$\dot{\omega_m}$ Derivative of mechanical speed

$\widehat{\dot{i_{\alpha,\beta}}}$ Derivative of current in $\alpha\beta frame$ - observed value

$\dot{i_{\alpha,\beta}}$ Derivative of current in $\alpha\beta$ frame

$\lambda_a, \lambda_b, \lambda_c$ Flux linkages in a, b and c phases

λ_f Rotor permanent magnet flux

$\lambda_{\alpha 0}, \lambda_{\beta 0}$ Initial condition of flux linkage in α and β axis

$\lambda_{\alpha f}, \lambda_{\beta f}$ Flux linkage in α and β axis

ω_e Motor electrical speed

ω_m Motor mechanical speed

ω_{drum} Washing machine drum mechanical speed

θ_r Rotor electrical position angle

$\widehat{\dot{\omega_m}}$ Derivative of mechanical speed - observed value

$\widehat{\omega_m}$ Mechanical speed - observed value

$\widehat{\omega_{e-smo}}$ Motor electrical speed from SMO method - observed value

$\widehat{\theta_{r-pll}}$ Rotor electrical position angle from PLL block - observed value

$\widehat{\theta_{r-smo}}$ Rotor electrical position angle from SMO method- observed value

$\widehat{e_{\alpha,\beta}}$ Back-emf in α and β axis - observed value

$\widehat{i_{\alpha,\beta}}$ Current in $\alpha\beta$ frame - observed value

$\widehat{i_{\alpha-ELO}}$, $\widehat{i_{\beta-ELO}}$ Current in α and β from ELO method - observed value

$\widehat{T_l}$ Load torque - observed value

$\widehat{w_{e-pll}}$ Motor electrical speed from PLL block - observed value

B Dumping coefficient

C Frictional Torque

e_α, e_β Back-emf in α and β axis

g Gravitational acceleration

i_α, i_β Currents in α and β axis

i_a, i_b, i_c Currents in a, b and c phases

i_d, i_q Currents in d and q axis

i_{dref}, i_{qref} Reference currents in d and q axis

i_{smax} Total current limit

J_l Load inertia

J_m Motor inertia

J_{eq} Equivalent inertia

L_d, L_q d and q axis inductances

L_s Synchronous inductance

m_{ubl} Mass of unbalanced load

P Pole numbers

P_i Input power expression in dq axis variables

P_{abc} Input power expression in abc variables

R_s Stator winding resistance

r_{drum} Washing machine drum radius

T_e Electromagnetic torque

T_l Load torque

T_{drum} Washing machine drum total torque

T_{e-reac} Reaction torque

T_{e-rlc} Reluctance torque

v_α, v_β Voltages in α and β axis

v_a, v_b, v_c Voltages in a, b and c phases

v_d, v_q Voltages in d and q axis

$v_{\alpha ref}, v_{\beta ref}$ Reference voltages in α and β axis

v_{dref}, v_{qref} Reference voltages in d and q axis

v_{sm} Available voltage margin

v_{sref} Total voltage reference

w_{ref} Motor electrical speed reference

$\widehat{\omega_{e-ELO}}$ Motor electrical speed from ELO method - observed value

$\widehat{\theta_{r-ELO}}$ Rotor electrical position angle from ELO method - observed value

CHAPTER I

INTRODUCTION

Energy efficiency and airborne acoustic noise are some of the main characteristics in household appliances for both end user and legislative directives. In addition to this, manufacturers should also care about the maintenance requirements of the appliance in lifetime. For a washing machine, motor is the one of most important areas to work for improving these characteristics. The PMSM popularity is increasing in washing machines over the conventional universal motors due to low maintenance requirement, lower acoustical noise level and simpler structure with absence of windings and brush/collector system in rotor. Also, PMSM has the energy efficiency and power density advantages compared with both universal and AC induction motors[2, 3]. Washing machines are a good application area of both variable loads and low-high speed operations. Loads are distributed in the drum of the washing machine in an unpredictable way due to nature of laundries. Usually some amount of the load is stacked to a point of the drum above a certain speed. This causes to an unbalanced load for the motor and resulted in sinusoidal varied load torque according to drum angular position. If the motor torque in the system can't trace this load torque, mechanical transmission parts of the machine wear out from torsional forces. Also, washing machine results in excess acoustical noise due to incident speed variation and unnecessarily high energy consumption [4, 5]. In sensorless FOC algorithm of PMSM, PI controllers are used in speed-current cascaded structure. The main advantages of traditional PI controller are its simplicity and its ability to ensure zero steady state error in stable systems. As a drawback, transient performance of PI controller suffers from external disturbances as variable unbalanced loads

of washing machines [6, 7, 8]. Another point is that, speed and rotor position information is needed in FOC algorithm. Sensorless approach has many advantages over the application with sensors in terms of cost, durability and lifetime. Speed and position information of sensorless approaches are synthesized from measured system parameters with a feedback system including a gain in both observer and tracing algorithms. In the both sensorless methods and applications with sensors, the measured parameters need a filtering for disturbances before to be used by the control system. This filtering limits the PI regulator's operating bandwidth. Therefore, PI controller starts having hard time to keep track of the time varying system parameters.

Regarding to sensorless control of the PMSM, many algorithms have been studied over the years. The speed and position estimators can be divided into two groups. The first group is high frequency signal injection based methods, which are effective at low speeds. However, for washing machine it is crucial to operate at high speed in water extraction phase. Also, this method requires a high computational effort for the microcontroller unit. Second group is back electromotive force (back-emf) based estimator methods, which are effective at high speed operation. Since the back-emf is very low at low speed, this method requires open loop startup algorithms. The back-EMF approaches are the popular and more attractive category for washing machines. There are many approaches to estimate back-emf of motors. There are linearization and stochastic based state observers as Extended Luenberger Observer (ELO) and Extended Kalman Filter (EKF) approaches. The computational burden for these methods is similar with high frequency injection method. Direct Integration Method which is basically a flux linkage estimators and sliding mode observers(SMO) can be a good choice to implement for washing machine motors thanks to their insensitivity to parameter variations, external disturbance rejection and fast dynamic response. For comparing the performances to be used in both sensorless motor control alghorithm and in proposed feedforward compensation with load torque observer Direct Integration, SMO and ELO methods

have been studied in this paper. Then, the load torque observer design is studied to improve PI controller performance. Feedforward compensation is built to improve the performance of washing machine with unbalanced load. Since the load torque observer design requires the motor speed information, it is crucial to have accurate results from sensorless speed and rotor position algorithm.

Rest of the paper is organized as follows, in chapter 2 an overview of the PMSM mathematical model and equations of motion including torque expressions of washing machine is reviewed. Field Oriented Control with Maximum torque Per Amper Strategy and Field Weakening are introduced in chapter 3. Sensorless motor speed and rotor position algorithms are studied in chapter 4. Direct Integration Method which is based on flux linkage estimator is given with feedback improvement. Sliding mode observer is presented with super-twisting and phase locked loop (PLL) algorithms. Also Extented Luenberger Observer with feedback linearization is presented. In chapter 5, a load torque observer design is constructed by the dynamic system equations. Two different algorithms are presented. In chapter 6, simulation and experimental results are discussed. Finally, in chapter 7, conclusion is presented.

CHAPTER II

SYSTEM MODELLING

2.1 Permanent Magnet Synchronous Motors Model

2.1.1 Permanent Magnet Synchronous Motor

Permanent Magnet Synchronous Motor(PMSM) is constant speed machine that always rotates in a constant speed which depends on the supply frequency. They are electronically commutated and sequentially driven by means of AC voltages. Rotor magnetic flux is gained with permanent magnets in these types of motors. PMSM can be classified in terms of many features. They can be inner or outer rotor structures. For washing machine applications, while inner type rotor structure is preferred in pulley-belt driven system, outer type rotor structure is preferred in direct drive applications.

Stator structure may either have distributed or concentrated windings. Concentrated winding types have several advantages over the distributed types as high power and torque density, high efficiency, short end turns, flux weakening capability, easy structure, high slot fill factor and system cost [9].

PMSMs can also be classified in terms of rotor structure. If the magnets are mounted on the surface of rotor it is called surface-mounted PMSM (SPMSM). This topology results in low torque ripple and smooth performance. The other variation of the PMSM is interior PMSM (IPMSM) which permanent magnets are buried inside the rotor. In this type of motors reluctance torque has the role of increasing the electromagnetic torque.

2.1.2 Mathematical Modelling of PMSM

2.1.2.1 Stator voltage equations and reference frame transformations

The stator voltage equation of the PMSM with phase variables can be written as follows [10]:

$$v_a = R_s i_a + \frac{d\lambda_a}{dt} \tag{2.1}$$

$$v_b = R_s i_b + \frac{d\lambda_b}{dt} \tag{2.2}$$

$$v_c = R_s i_c + \frac{d\lambda_c}{dt} \tag{2.3}$$

Both voltage and current in above equation are sinusoidally varied parameters and non-linear. Therefore mathematical model in phase quantities is not usually convenient for control.It needs to be transform in stationary and rotary reference frames.

Mathematical Clarke Transform and stator voltage equations in stationary frame

The mathematical transformation called Clarke Transform modifies a three phase system to a two phase orthogonal system $\alpha\beta$ frame:

$$v_\alpha = \frac{2}{3} v_a - \frac{1}{3}(v_b - v_c) \tag{2.4}$$

$$v_\beta = \frac{1}{\sqrt{3}}(v_a + 2v_b) \tag{2.5}$$

$$v_0 = \frac{2}{3}(v_a + v_b + v_c) \tag{2.6}$$

If the PMSM drive system is considered three phase balanced system, the homopolar component v_0 is absent. The stator voltage equations in stationary frame can be expressed as follows:

$$v_\alpha = R_s i_\alpha + L_s \frac{d i_\alpha}{dt} - \lambda_f sin\theta_r \omega_e \tag{2.7}$$

$$v_\beta = R_s i_\beta + L_s \frac{d i_\beta}{dt} + \lambda_f cos\theta_r \omega_e \tag{2.8}$$

Mathematical Park Transform and stator voltage equations in rotary frame

The two phases $\alpha\beta$ frame representation calculated with the Clarke Transform is then fed to a vector rotation block where it is rotated over an angle θ_r to follow the frame d,q attached to the rotor flux.

The rotation over an angle θ_r is done according to following formula:

$$v_d = v_\alpha \cos\theta_r + v_\beta \sin\theta_r \tag{2.9}$$

$$v_q = -v_\alpha \sin\theta_r + v_\beta \cos\theta_r \tag{2.10}$$

The stator voltage equations in rotary frame can be expressed as following:

$$v_d = R_s id + L_d \frac{di_d}{dt} - \omega_e L_q i_q \tag{2.11}$$

$$v_q = R_s iq + L_q \frac{di_q}{dt} + \omega_e L_d i_d + \lambda_f \omega_e \tag{2.12}$$

Mathematical Inverse Park and Clarke transforms

The vector in the rotary frame is transformed to the two phases $\alpha\beta$ stationary frame representation calculated with a rotation over an angle θ_r according to following formula:

$$v_\alpha = v_d \cos\theta_r - v_q \sin\theta_r \tag{2.13}$$

$$v_\beta = v_d \sin\theta_r + v_q \cos\theta_r \tag{2.14}$$

The modification from $\alpha\beta$ stationary stationary frame to a three-phase system variables is given in the following equations:

$$v_a = v_\alpha \tag{2.15}$$

$$v_b = \frac{\sqrt{3}v_\beta - v_\alpha}{2} \tag{2.16}$$

$$v_c = -\frac{\sqrt{3}v_\beta - v_\alpha}{2} \tag{2.17}$$

It should be noted that all mathematical formulas for Clarke, Park and their inverse transformation forms are also applicable to stator current variables.

2.1.2.2 Torque expressions and dynamic system equations

The input total instantaneous power of a three phase PMSM system may be expressed in abc variables as follows;

$$P_{abc} = v_a i_a + v_b i_b + v_c i_c \tag{2.18}$$

The input power equation can be expressed with the appropriate Clarke-Park Transforms.

$$P_i = \frac{3}{2}(v_q i_q + v_d i_d) \tag{2.19}$$

The equation for input power is given by (2.19) and the electromagnetic torque multiplied by the rotor mechanical angular velocity is the power output. As a result we have the following expression

$$T_e \frac{2}{P}\omega_e = \frac{3}{2}(v_q i_q + v_d i_d) \tag{2.20}$$

Substituting (2.9)–(2.10) into (2.20) results

$$T_e = \frac{3}{2}\frac{P}{2}[i_q \lambda_f + (L_d - L_q) i_q i_d] \tag{2.21}$$

Torque expression in (2.21) can be analized in two parts. The first component of the electromagnetic torque is called reaction torque and it is generated by the interaction

between rotor and stator magnetic fields. The reaction torque is expressed as follows:

$$T_{e-reac} = \frac{3}{2}\frac{P}{2}(i_q \lambda_f) \tag{2.22}$$

The second component of the electromagnetic torque is called reluctance torque and it is generated as a result of a magnetic field trying to minimize the reluctance of its fluxpath. The reluctance torque is expressed as follows:

$$T_{e-rlc} = \frac{3}{2}\frac{P}{2}(L_d - L_q) i_q i_d \tag{2.23}$$

It should be noted that in general SPMSM motors $L_d = L_q$. Therefore there is no any reluctance torque in SPMSM. Then (2.23) yields to a result that, there is no need to impose any i_d current to stator winding if field weakening operation is not needed. Therefore rotor/stator magnetic field alignment should be kept in 90^o degrees.

Magnet orientation in rotor results in L_d, L_q difference in IPMSM motors. This difference yields to a result that an optimum electrical degree should be find in rotor/stator magnetic field alignment for the maximum torque. As it can be seen in figure 1 rotor/stator magnetic field alignment angle is beyond the 90^o degrees.

Most electric motors are of rotating type and coupled with a load. In the example of washing machine system, both direct drive and pulley-belt driven systems, motor produces electromagnetic torque T_e to rotate the desired load. In most systems, we can assume that the rotating part of the motor with inertia J_m is coupled to the load inertia J_l. The net torque (difference between electromagnetic torque and load torque) over the equivalent inertia, causes to acceleration or deceleration of the load in accordance with the following rotating system dynamic equation [11]:

$$\frac{d\omega_m}{dt} = \frac{(T_e - T_l)}{J_{eq}} \tag{2.24}$$

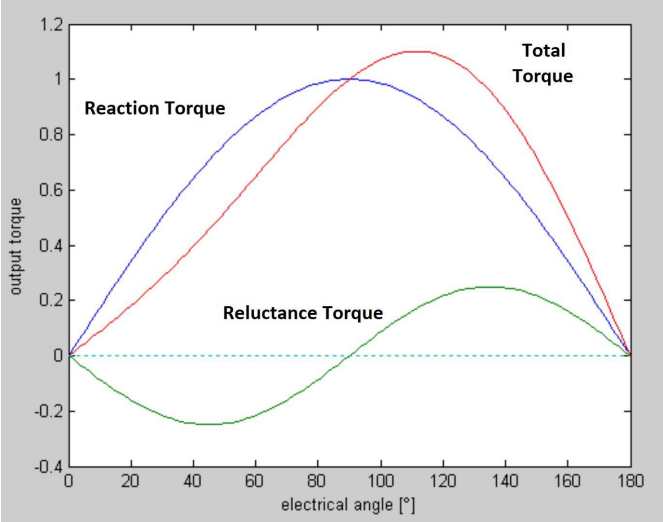

Figure 1: Torque characteristic for an IPMSM.

It is considered that T_l consists the bearing friction, wind resistance(drag) and damping forces. Equivalent inertia J_{eq} is the sum of J_m and J_l.

Washing machine dynamic equation

Horizontal axis washing machines (front loading) is a good application area for driving systems with wide operation speed range and torque requirement. Washing machines has a drum for the wash operation and uses motor agitations to maintain a washing performance. In low speed washing and rinsing mode drum speed is kept around 0-80 rpm. In this phase load is usually unpredictable and requires high and variable torque. Therefore control system should be implemented to keep track this load in a reliable manner. Water extraction phase (spinning) starts above the 80 rpm and laundries in drum start to stack in drum of the washing machine. Washing machine can reach 1600 and even 2000 rpm speeds in this spinning phase. Therefore, if the laundries are not distributed in a balanced way, risky conditions can occur due to centrifugal forces. Washing machine can start to vibrate and walk. So this situation can even lead to machine break down.Figure 2 illustrates the general view of washing machine and figure 3

illustrates a view of washing machine with unbalanced load. Field weakening called algorithms should be used to meet washing machine wide speed operation requirements. Washing machine general rotational system equation can be expressed as follows for above 80 rpm speed:

$$T_{drum} = J_{eq}\frac{d\omega_{drum}}{dt} + m_{ubl}gr_{drum}\sin w_{drum}t + B\omega_{drum} + C \tag{2.25}$$

There are four types of torque in equation (2.25). Inertial torque, which is related with J_{eq} occurs in acceleration or deceleration phase of the drum. Damping torque, which is related with B is disregarded compared with other types of torques. Friction torque which is illustrated with C occurs from belt, bearing, laundry friction etc. and disregarded compared with other torques. Potential torque which is related with m_{ubl} is the torque caused by unbalanced load and the main part of the load torque in washing machine applications. It should be noted that, there is a sinusoidally varied load torque to drive in washing machine application above certain speed.

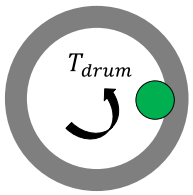

Figure 2: Drum torque in washing machine.

Figure 3: Washing Machine with unbalanced load

CHAPTER III

FIELD ORIENTED CONTROL OF PMSM

3.1 Field Oriented Control (FOC)

As described in section 2.1.2, PMSM motors are driven by sinusoidally varied stator currents and for controlling a load profile with a desired speed profile, it is required to control currents in stator windings. By the help of increasing process abilities in the microcontrollers, it is possible to implement advanced control strategies, which use mathematical clark and park transformations in order to decouple the torque generation and the magnetization functions in PM motors. In the example of separately exited DC motors, it is possible to control torque and flux independently. By controlling the field winding current it possible to control the flux and the current through the rotor windings determines how much torque is produced. Collector and brush construction of these motors guarantees that field and armature magnetic fluxes always perpendicular to each other. In field oriented control of PMSM by the help of Clarke and Park Transformations it is possible to control magnetic flux and motor torque independently by d and q axis currents as in separately exited DC motors. As it can be seen in figure 4 d and q axis currents rotates with the total current vector i_s. Therefore with the help of these mathematical transformations, system parameters are now DC values. It should be noted that for performing equations (2.9), (2.10) and (2.13), (2.14) rotor position information θ_r is required.

The control diagram in figure 5 summarizes the closed loop FOC of the PMSM. The control diagram is a speed-current (torque and flux) cascaded structure. It is essential to measure stator currents and motor speed to be used in feedback system. Also rotor position information is the core of FOC for the transformations. FOC alghoritm allows

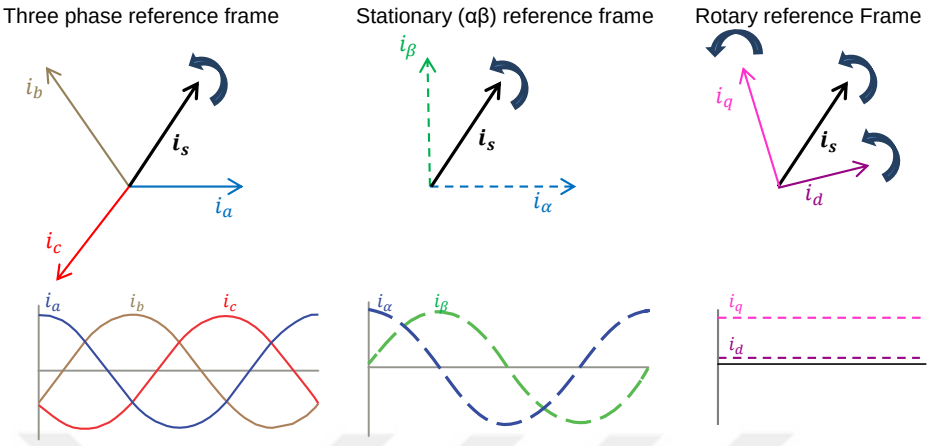

Figure 4: Reference frames in FOC algorithm

us to control motor torque and flux in each sampling state of the microcontroller. This control flexibility is crucial for washing machine operation which system has variable load torque and speed requirements.

For current measurement, hardware components as hall effect sensors or shunt resistances can be used. For measuring the speed and rotor position informations even there are hardware sensor methods as hall sensors or encoders, it is possible to construct a sensorless scheme.

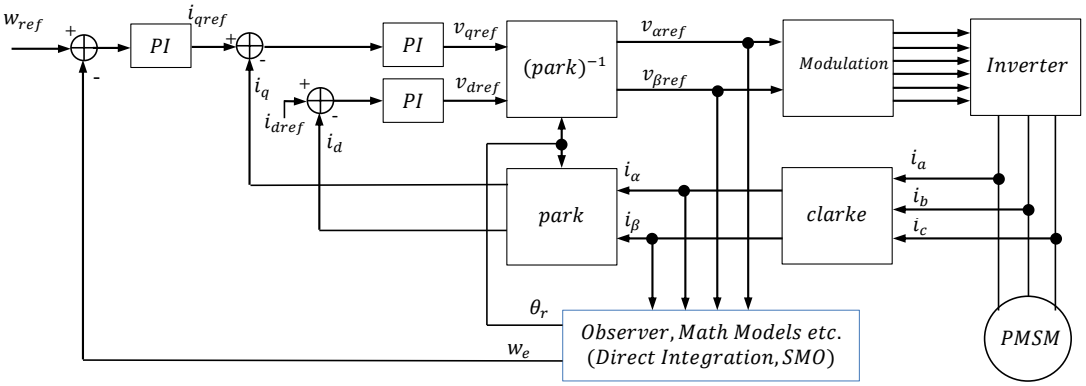

Figure 5: Field oriented control of PMSM

In this scheme firstly, motor phase currents are measured. These measurements are fed to the Clarke and Park Transformation modules. The outputs of this projection gives the current in the d,q rotating reference frame. The i_d and i_q components are compared with the references i_{dref} (the flux reference) and i_{qref} (the torque reference). The torque is required for acceleration or decelaration of motor. Thereby, the torque reference is the output of speed control block. The flux reference will be described in section 3.2 and 3.3. For measuring speed, observer models are indicated to describe sensorless scheme in figure 5. Measured electrical speed w_e is compared with the speed reference w_{ref}. In both speed and current blocks, error is amplified with a PI control. At the end, by using Inverse Park or Clarke Transformations voltage references are fed to modulation block. For modulation, by using sinusoidal PWM, space vector PWM or clamped PWM modulation etc. sinusoidal voltages for winding to be applied can be found. In FOC algorithm of PMSM, PI controllers are used in speed-current cascaded structure. The main advantages of traditional PI controller are its simplicity and its ability to ensure zero steady state error in stable systems.

In following two sections, maximum torque per amper (MTPA) and field weakening (FW) algorithms are described. In the example of washing machine, in washing and rinsing phases, it is required to have maximum torque. Energy efficiency is one of the main characteristics in household appliances for both end user and legislative directives. Therefore MTPA is used to find optimum control to get maximum efficiency. In spinning phase, for reducing the back electromotive force (back-emf) voltage of PMSM, it is required to use negative i_d current. FW algorithm is used to handle high back-emf voltage in the FOC of PMSM.

3.2 Maximum Torque Per Amper Strategy (MTPA)

The MTPA control is a strategy which maximize electromagnetic torque while using the minimum stator current magnitude. There are infinite numbers of i_d and i_q combinations which can produce the same amount of torque. MTPA algorithm aims to find minimum total current vector. By doing this the copper losses are minimized, and the overall efficiency of the motor can be increased [12].

As described in section 2.1.2.2 L_d and L_q difference of IPMSM motors requires rotor/stator magnetic field alignment angle beyond 90^o degrees. Since permanent magnets have higher reluctance than iron, inductance along the d axis is usually lower than that along the q axis [10]. As a result, in IPMSMs, L_d is smaller than L_q. This yields to a requirement of negative i_d current for reluctance torque production.

In order to find minimum stator current for a defined torque value, equation (2.21) is used.

$$T_e = \frac{3}{2}\frac{P}{2}[i_q\lambda_f + (L_d - L_q)i_q i_d]$$

In all inverter systems there is a limitation of the stator current, due to the physical current limitation. By adding this constraint in the system, following equation is obtained.

$$i_{smax}{}^2 = i_d{}^2 + i_q{}^2 \tag{3.1}$$

By representing i_q in (2.21)with the stator current i_{smax} in equation (3.1),

$$T_e = \frac{3}{2}\frac{P}{2}[\lambda_f\sqrt{i_{smax}{}^2 - i_d{}^2} + (L_d - L_q)i_d\sqrt{i_{smax}{}^2 - i_d{}^2}] \tag{3.2}$$

In order to find the minimum i_d current that satisfies the torque equation, the electromagnetic torque T_e can be derivated with respect to i_d.

$$\frac{dT_e}{di_d} = \frac{3}{2}\frac{P}{2}\frac{-i_d\lambda_f + (L_d - L_q)(i_{smax} - 2{i_d}^2)}{\sqrt{{i_{smax}}^2 - i_d^2}} \tag{3.3}$$

From this equation the minimum i_d current for the desired torque is found as follows:

$$i_d = \frac{-\lambda_f + \sqrt{\lambda_f^2 + 8(L_d - L_q)^2 {i_{smax}}^2}}{4(L_d - L_q)} \tag{3.4}$$

From the equation (3.1) q axis current i_q can be found.

$$i_q = \sqrt{{i_{smax}}^2 - {i_d}^2} \tag{3.5}$$

3.3 Field Weakening Strategy (FW)

In motor control systems, if the wide speed operation is required, the extended motor speed exposes some technical challenges. As described in section 3.2, due to the upper limit of dc link voltage and current ratings of the inverter, the motor input voltage and current ratings are limited. If the equations (2.11) and (2.12) recalled below,

$$v_d = R_s id + L_d\frac{di_d}{dt} - \omega_e L_q i_q$$

$$v_q = R_s iq + L_q\frac{di_q}{dt} + \omega_e L_d i_d + \lambda_f \omega_e$$

The voltage term $\lambda_f\omega_e$ grows up with the speed, imposing a limit to the maximum reachable speed, due to the limited voltage availability. It should be noted that the motors with high back-emf resulted in higher torque with same current. But they can work only at lower speed. Motors which designed for higher speed are made with lower back-emf resulted in lower torque with the same current. In the example of washing machines operation, it is necessary to have high torque with low current at low speed of washing and rinsing operation , but also motor needs to reach higher speeds in spinning phase (even if with a reduction of the torque/current ratio). In such cases flux weakening strategy can be applied to expend speed range of the PMSM.The idea in this strategy is using the d axis current to create a q axis voltage. If the equation (2.12) rearranged,

$$v_q = R_s i q + L_q \frac{d i_q}{d t} + \omega_e (L_d i_d + \lambda_f) \tag{3.6}$$

It can be noticed that, a negative set of i_d reduces the back-emf term and increasing the reachable speed.

The common method for generating negative i_d current start with calculating reference voltage amplitude as follows:

$$v_{sref} = \sqrt{(v_{dref}^2 + v_{qref}^2)} \tag{3.7}$$

Then the available voltage margin v_{sm} is computed with maximum allowed inverter voltage vector amplitude v_{smax}.

$$v_{sm} = K_m v_{smax} - v_{sref} \tag{3.8}$$

K_m is a constant gain, generally equal to 0.9. At the end for generating the negative i_d current following conditional equation can be used:

$$i_{dref} = \begin{cases} \Sigma K_g v_{sm}, & \text{if } v_{sm} \leq 0 \\ i_{dref-MTPA}, & \text{otherwise} \end{cases}$$

If available voltage margin is a negative value, then the i_{dref} can be increased in each control step of the drive algorithm with a certain K_g gain until voltage margin turns back to normal. Another method that uses an integrator with anti-windup is demonstrated in figure 6 below [1],

In this scheme the firstly the voltage margin v_{sm} is calculated and fed to integrator with anti-windup. The output of this integrator is field weakening coefficient β_q. β_q which is limited between 0 and 1 is multiplied with the complementary angle of the stator current vector i_s. When the K_{fw} and K_{aw} coefficients are tuned, if the voltage margin v_{sm} is negative, the output of the integrator decrease below 1. This will result

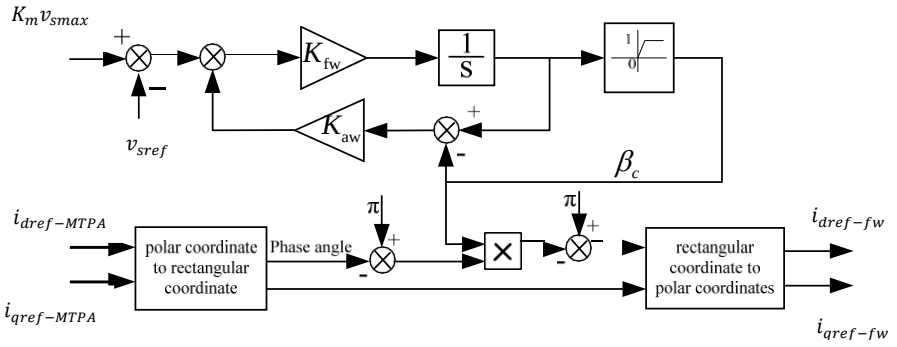

Figure 6: Control block diagram for the field weakening algorithm[1].

an increase in the last phase angle after the calculation. Therefore a negative i_{dref} will be imposed. If the voltage margin v_{sm} increase to a positive value, β_q will immediately increase to 1 and phase angle from MTPA algorithm will not be changed.

CHAPTER IV

SENSORLESS SPEED AND ROTOR POSITION ESTIMATION SCHEMES

As described in section 3.1 rotor position information is crucial for the FOC algorithm. Motor speed is also required for the closed loop control. Even if hardware sensor methods can be used, sensorless approach has many advantages over the application with sensors in terms of cost, durability and lifetime. Speed and position information of sensorless approaches are synthesized from measured system parameters with a feedback system including a gain in both observer and tracing algorithms.

In this study, three back-emf based estimator methods are investigated for the performance in the washing machine operation. These methods are Extended Luenberger Observer, Direct Integration Method and Sliding Mode Observer.

4.1 Direct Integration Method

Integration based flux linkage estimator suffers from the integral operation. Integration operation is not an easy task for a microcontroller due to initial conditions, noise and measurement offsets. In order to improve the integration operation performance, a feedback signal is used for correction in integral method. Rotor magnetic fluxes in $\alpha\beta$ reference frame are extracted from motor model equations.

When the stator voltage eqution in stationary frame (2.7) and (2.8) examined, it can be seen the rotor position information θ_r is hidden in these equations. ($\lambda_f sin\theta_r\omega_e$ and $\lambda_f cos\theta_r\omega_e$). It is possible to extract magnetic fluxes in α β frames as follows [13, 14]:

$$\lambda_{\alpha f} = \lambda_{\alpha 0} + \int_0^t (v_\alpha - R_s i_\alpha) dt - L_s i_\alpha \tag{4.1}$$

$$\lambda_{\beta f} = \lambda_{\beta 0} + \int_0^t (v_\beta - R_s i_\beta) dt - L_s i_\beta \tag{4.2}$$

Where $\lambda_{\alpha f}$ and $\lambda_{\beta f}$ is α β components of rotor permanent magnet flux, $\lambda_{\alpha 0}$ and $\lambda_{\beta f}$ are initial conditions. Extracted magnetic fluxes were corrected with feedback gained control scheme. In this approach, rotor magnet flux is considered to be known from manufacturer datasheet or with measurement. A gain G is used with a feedback for error between calculated parameter and rotor magnet flux. Then the rotor position is derived from the following equation:

$$\theta_r = tan^{-1}(\frac{\lambda_{\alpha f}}{\lambda_{\beta f}}) \tag{4.3}$$

The motor speed can be estimated from the time differentiation of equation (4.3):

$$\omega_e = \frac{d\theta_r}{dt} \tag{4.4}$$

Figure 7 shows a block diagram of direct integration method with feedback.

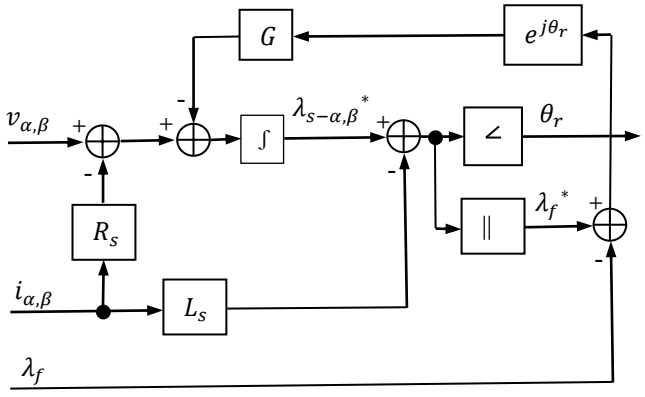

Figure 7: Direct integration method with feedback block diagram.

4.2 Sliding Mode Observer

In other estimation technique, sliding mode observer design is studied. In this method, error between reference and measured parameter is kept in the sliding surface with high

gained control signals. In the real application, even sliding mode control is considered to be robust to disturbances including measurement noise, it is suffered from saturation, but for observer schemes there is no limitation in the MCU and thereby numerical calculations. Sliding mode observer for rotor position and speed information is constructed from motor model equations as follows:

$$\dot{i_{\alpha,\beta}} = \frac{v_{\alpha,\beta} - R_s i_{\alpha,\beta} - e_{\alpha,\beta}}{L_s} \tag{4.5}$$

$$\dot{\widehat{i_{\alpha,\beta}}} = \frac{v_{\alpha,\beta} - R_s \widehat{i_{\alpha,\beta}} + Ksign(\widehat{i_{\alpha,\beta}} - i_{\alpha,\beta})}{L_s} \tag{4.6}$$

$$\dot{\widehat{i_{\alpha,\beta}}} - \dot{i_{\alpha,\beta}} = -R_s \widehat{i_{\alpha,\beta}} + R_s i_{\alpha,\beta} + Ksign(\widehat{i_{\alpha,\beta}} - i_{\alpha,\beta}) + e_{\alpha,\beta} \tag{4.7}$$

Where e_α and e_β is the back-emf components defined from equations (2.7) and (2.8) as follows:

$$e_\alpha = -\lambda_f \sin\theta_r \omega_e \tag{4.8}$$

$$e_\beta = \lambda_f \cos\theta_r \omega_e \tag{4.9}$$

Sliding mode surface is chosen as $s = \widehat{i_{\alpha,\beta}} - i_{\alpha,\beta}$ and $\dot{s} = \dot{\widehat{i_{\alpha,\beta}}} - \dot{i_{\alpha,\beta}}$. The sliding mode occurs with sufficiently large switching gain K. The system enters the sliding mode motion when $s = 0$ and $\dot{s} = 0$. From the equivalent control method $\widehat{e_{\alpha,\beta}}$ is obtained as follows:

$$\widehat{e_{\alpha,\beta}} = -Ksign(\widehat{i_{\alpha,\beta}} - i_{\alpha,\beta}) \tag{4.10}$$

The rotor position is derived from:

$$\widehat{\theta_{r-smo}} = tan^{-1}(\frac{\widehat{e_\alpha}}{\widehat{e_\beta}}) \tag{4.11}$$

Motor electrical speed can be estimated as in the equation (4.4):

$$\widehat{\omega_{e-smo}} = \frac{d\widehat{\theta_{r-smo}}}{dt} \tag{4.12}$$

Nevertheless, sliding mode observer uses high frequency and high gains to keep the system in sliding surface. This method leads to undesirable phenomenon of oscillations having finite frequency and amplitude, which is known as chattering [15, 16]. In the end, this method requires a heavy filtering before to be used in control algorithms. Therefore, instead of using a discontinuous sign function, a sigmoid function or super-twisting called algorithms which continuous function of time can be used to obtain a smoother switching. A smoother switching can occur without compromising the robustness properties by using continuous switching action. In this study super-twisting algorithm is chosen after literature study [17]. The control algorithm in this method is defined by the following control law:

$$u = \delta\sqrt{|s|}sign(s) + m \tag{4.13}$$

$$\dot{m} = -Msign(s) \tag{4.14}$$

Where δ and M are positive constants to be tuned in the system. The super-twisting algorithm can be seen as nonlinear version of PI controller as it can be seen from the figure below.

Equation (4.10) is redesigned with u parameter from the super-twisting algorithm as follows:

$$\widehat{e_{\alpha,\beta}} = \delta\sqrt{|s|}sign(\widehat{i_{\alpha,\beta}} - i_{\alpha,\beta}) + m \tag{4.15}$$

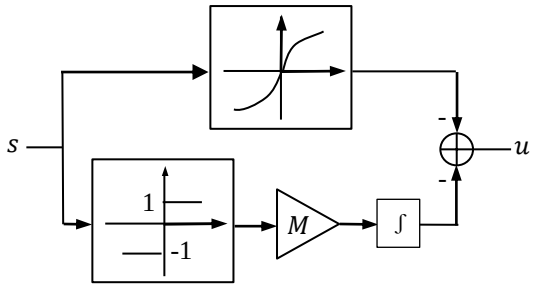

Figure 8: Super-twisting alghorithm block diagram.

The common method of rotor position and speed calculation is given in equations (4.11) and (4.12). Speed is obtained with derivation of the rotor position. However, calculated precision in such a way is not high and a small deviation or noise of estimated rotor position can cause a large deviation of speed error. For this problem, the common way used is low-pass filter for filtering. However, low-pass filter doesn't have a good performance in reducing speed error and also causes to phase shift. Phase locked loop algorithm is used with super-twisting algorithm for eliminating the chattering effect with minimal need of low-pass filter [16]. The block diagram of speed and rotor position estimation based on PLL can be shown as in figure 9.

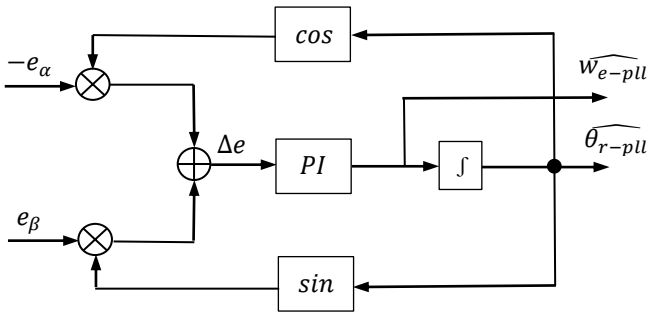

Figure 9: PLL block diagram.

From equations (4.8) and (4.9) Δe in figure 9 can be obtained as follows:

$$\Delta e = -e_\alpha \cos\theta_r - e_\beta \sin\theta_r \tag{4.16}$$

$$\Delta e = \lambda_f \widehat{w_{e-smo}} \sin(\widehat{\theta_{r-pll}}) \cos(\widehat{\theta_{r-smo}}) - \lambda_f \widehat{w_{e-smo}} \cos(\widehat{\theta_{r-pll}}) \sin(\widehat{\theta_{r-smo}}) \tag{4.17}$$

$$\Delta e = \lambda_f \widehat{w_{e-smo}} \sin(\widehat{\theta_{r-pll}} - \widehat{\theta_{r-smo}}) \tag{4.18}$$

Subscripts pll represents the estimated rotor position and motor electrical speed from PLL block. If the error Δe can be controlled to be zero, the estimated motor electrical speed can be obtained with a PI control as follows:

$$\widehat{w_{e-pll}} = k_{p-pll} \Delta e + k_{i-pll} \int \Delta e dt \tag{4.19}$$

Finally, the rotor position cab be obtained as follows:

$$\widehat{\theta_{r-smo}} = \int \widehat{w_{e-pll}} dt \tag{4.20}$$

4.3 Extended Luenberger Observer

A state observer is an algorithm implemented to reconstruct the inaccessible states in a system using accessible states. Accessible states for PMSM are the components of stator currents and voltages. The most commonly used state observers are Luenberger and Kalman types. When compared with Luenberger, Kalman type is a stochastic method which uses both states and noise created by system measurement and modeling. However, this stochastic approach appears to have some inherent disadvantages. Difficulties may arise in situations where the noise content of the system and associated measurements are too low. In any case a normal state observer is only applicable to linear, time-invariant system. As it can be seen in state space equation of PMSM in equation (4.22) PMSM is a non-linear system. States i_d and i_q are multiplied by state ω_e. The Extended Luenberger Observer is a variation of a state observer which uses a linearized PMSM model. Therefore in every step, a linearization is required in extended state observers[18]. For linearization, derivation of jacobian matrix for state space equation in equation (4.22) is one of the methods. Then the observer poles shroud be determined. These steps should be repeated in every step of the control. All these calculations

are computational burden for MCU and hard to implement in unstable systems as washing machines. Therefore to overcome this, ELO with a feedback linerization technique is constructed[19]. Equations (2.7), (2.8) and following electromagnetic torque equation in α β stationary frames is used.

$$T_e = \frac{3}{2}\frac{P}{2}\lambda_f(-i_\alpha \sin\theta_r + i_\beta \cos\theta_r) \tag{4.21}$$

$$\begin{bmatrix} \widehat{\frac{d\theta_{r-ELO}}{dt}} \\ \widehat{\frac{d\omega_{e-ELO}}{dt}} \\ \frac{d\hat{i}_\alpha}{dt} \\ \frac{d\hat{i}_\beta}{dt} \end{bmatrix} = \begin{bmatrix} \widehat{\omega_{e-ELO}} \\ \frac{3}{2}\frac{P}{2J}\lambda_f(-\widehat{i_{\alpha-ELO}}\sin\theta_{r-ELO} + \widehat{i_{\beta-ELO}}\cos\theta_{r-ELO}) - \frac{B\widehat{\omega_{e-ELO}}}{J_e q} \\ -\frac{R_s}{L_s}\widehat{i_{\alpha-ELO}} + \frac{\lambda_f}{L_s}\widehat{\omega_{e-ELO}}sin\widehat{\theta_{r-ELO}} + \frac{v_\alpha}{L_s} \\ -\frac{R_s}{L_s}\widehat{i_{\beta-ELO}} - \frac{\lambda_f}{L_s}\widehat{\omega_{e-ELO}}sin\widehat{\theta_{r-ELO}} + \frac{v_\beta}{L_s} \end{bmatrix} + \Upsilon \begin{bmatrix} i_\alpha - \widehat{i_{\alpha-ELO}} \\ i_\beta - \widehat{i_{\beta-ELO}} \end{bmatrix} \tag{4.22}$$

with

$$\Upsilon = \begin{bmatrix} \Gamma K_{ELO} \end{bmatrix}$$

$$K_{ELO} = \begin{bmatrix} k_{11} & k_{12} \\ k_{21} & k_{22} \\ k_{31} & k_{32} \\ k_{41} & k_{42} \end{bmatrix} \quad \Gamma = \begin{bmatrix} \frac{L_s}{\lambda_f}\frac{\cos\widehat{\theta_{r-ELO}}}{\widehat{\omega_{e-ELO}}} & \frac{L_s}{\lambda_f}\frac{\sin\widehat{\theta_{r-ELO}}}{\widehat{\omega_{e-ELO}}} & 0 & 0 \\ \frac{L_s}{\lambda_f}\sin\widehat{\theta_{r-ELO}} & \frac{L_s}{\lambda_f}\cos\widehat{\theta_{r-ELO}} & 0 & 0 \\ 0 & 0 & 1 & 0 \\ 0 & 0 & 0 & 1 \end{bmatrix}$$

In this method, system is linerized using the Υ gain and known α β currents. So disadvantages of the jacobian method are eliminated. K is a gain matrix, Γ in equation (4.22) is the non-linear gain matrix and a compelling derivation of Γ is presented in [19]. By the help of equation (4.22), it is possible to extract $\widehat{\theta_{r-ELO}}$ and $\widehat{\omega_{e-ELO}}$ with a simple integration.

CHAPTER V

LOAD TORQUE OBSERVER

As described in chapter 1, a load torque observer design is studied to improve PI controller hence the washing machine driving performance. Feedforward compensation is built to improve the performance of washing machine with unbalanced load. The load torque observer design is constructed by system mechanical equations. Equivalent torque in a rotational system is proportional to system equivalent inertia and angular acceleration as it is demonstrated in equation (2.24).

System is able to calculate inertia as it is described in section 5.3 and electromagnetic torque in this scheme. Also, speed is obtained from the sensorless approach. Therefore, it is possible to construct an observer scheme to obtain unknown load torque parameter from the measured and calculated parameters. Since the only unknown parameter is the T_l in equation (2.24), an observer scheme is constructed as follows:

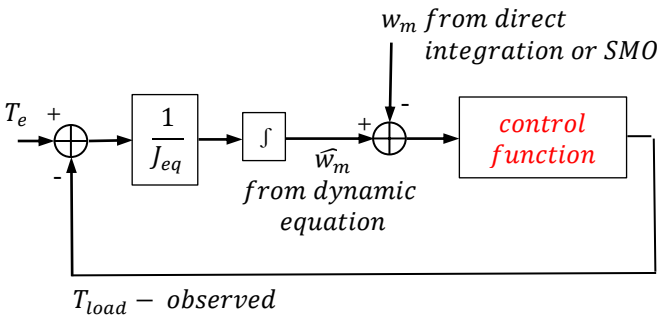

Figure 10: Load torque observer block diagram.

5.1 Load torque observer with SMO method

Error between observed and measured speed parameters is corrected with control function in figure 10. In this scheme for the control function, two different approaches were constructed. First, sliding mode observer is constructed as follows:

$$\widehat{\dot{\omega_m}} = \frac{T_e - K_{tl} sign(\omega_m - \widehat{\omega_m})}{J_{eq}} \tag{5.1}$$

Error equation can be obtained by subtracting (5.1) from (2.24):

$$\widehat{\dot{\omega_m}} - \dot{\omega_m} = \frac{T_l - K_{tl} sign(\widehat{\omega_m} - \omega_m)}{J_{eq}} \tag{5.2}$$

Sliding surface is chosen as $\dot{s} = \dot{\omega_m} - \widehat{\dot{\omega_m}}$ and $s = \omega_m - \widehat{\omega_m}$, with sufficiently large switching gain K_{tl}, the sliding mode occurs. The system enters the sliding mode motion when $s = 0$ and $\dot{s} = 0$. From the equivelent control method T_l is obtained as follows:

$$\widehat{T_l} = K_{tl} sign(\omega_m - \widehat{\omega_m}) \tag{5.3}$$

It should be noted that, in order to minimize chattering effect, super–twisting method should be implemented instead of above equation as explained in (4.13) and (4.13).

5.2 Load torque observer with PI control method

In sliding mode load torque observer, it is possible to have accurate results, but it suffered from the chattering in drawback. Since the obtained torque is used in the feed-forward compensation of PI controller, system will try to trace a noisy reference. This may cause severe damage in the mechanical transmission parts. So it is important to have a smooth torque reference in the PI controller. This is achieved by using the traditional PI gains for the control function in figure 10. Error between real and observed motor speed is referenced to be equal.

If PI is well tuned in the above figure real and observed motor speeds will be equal. Thus T_l will be obtained.

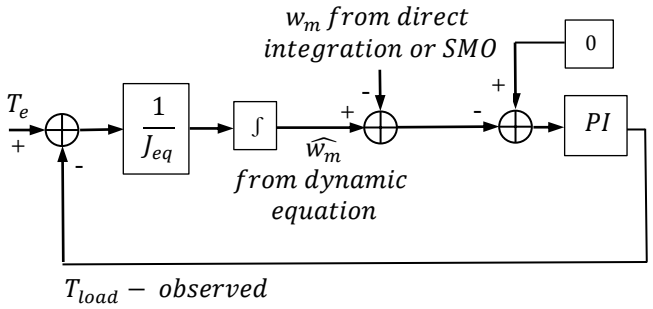

Figure 11: Load torque observer with PI gains.

5.3 Equivalent inertia calculation

For the load torque observer schemes in both SMO and PI gains, inertia information is required. In washing machine example, as described in section 2.1.2.2 laundries start to stack in drum above the 80 rpm. This behaviour of the washing machine leads to a constant equivalent inertia. Thus, it is possible to obtain an approximate equivalent inertia from the equation (2.24) with the following steps.

Step 1 Calculate the average electromagnetic torque in a constant speed

Step 2 Calculate the average electromagnetic torque in accelaration phase after steady state condition established

Step 3 Calculate the time and speed difference starting from acceleration command to destination speed

Step 4 Calculate the equivalent inertia with equation (2.24) by found parameters

In step 1 according to equation (2.25) since there is no any acceleration or deceleration, obtained torque can be accepted as T_l of the drum. In step 2 torque that increases the speed of the drum can be considered as the acceleration torque. Thus with step 3 and step 4 approximate equivalent inertia can be obtained.

At the end, by the addition of load torque observer improved FOC block diagram of washing machine can be found in following figure.

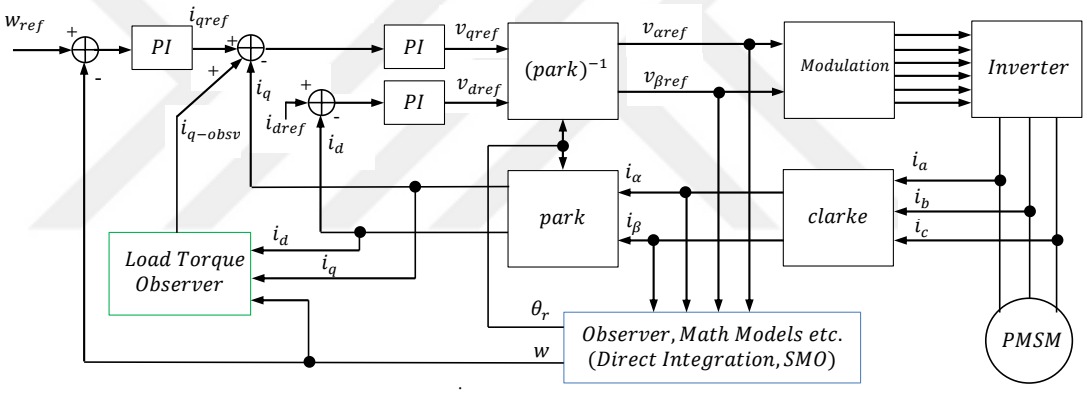

Figure 12: FOC block diagram with load torque observer.

CHAPTER VI

SIMULATIONS AND EXPERIMENTS

In order to verify the performance of the adopted sensorless schemes and load torque feedforward compensation, detailed simulations have been conducted. Firstly, ELO and Direct Integration Method is compared. A constant load of 0.5 Nm is applied as load torque with 1750 rpm motor speed reference. Figure 13 below illustrates the speed response of the system and figure 14 illustrates the torque response. Real motor speed and rotor position of the simulations are used in the feedback. Thereby, according to these figures, motor is able to control this system in a reliable manner. Observed torque is not used in the feedforward compensation. When the ELO and Direct Integration Observer Schemes speed responses are examined, even the steady state error is not existing but there are high frequency ripples in the system. In this constant load condition, ELO method has smaller ripples compared with the Direct Integration Method. When the figure 14 torque response of the system is examined, it can be found that, both motor electromagnetic torque and observed torque is able to track the real load profile.

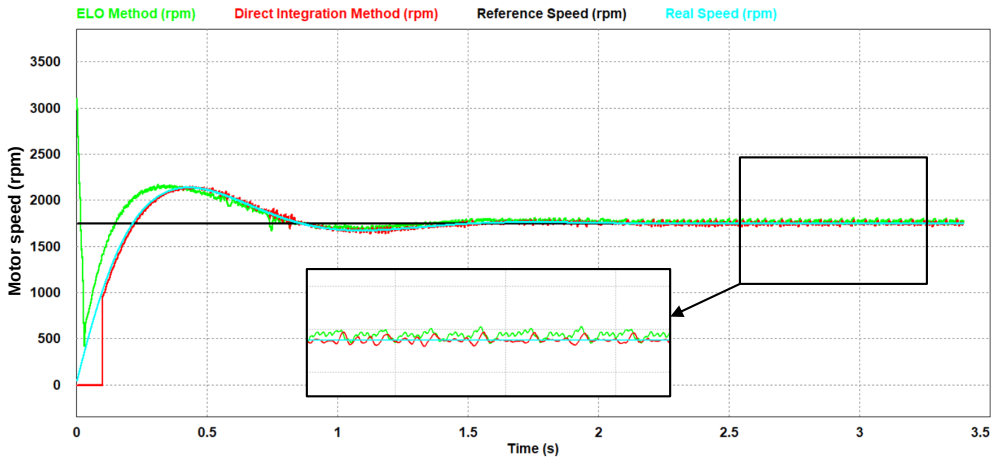

Figure 13: Speed response at constant load - ELO and Direct Integration Method comparison

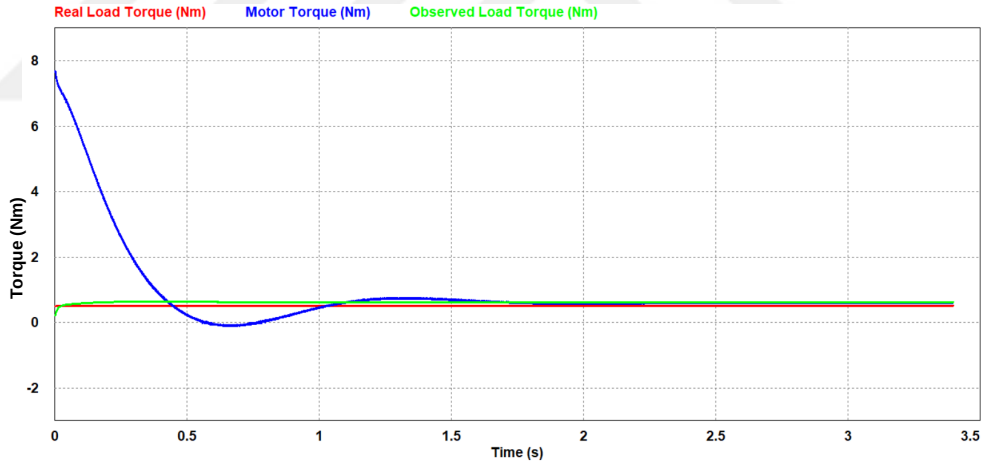

Figure 14: Torque response at constant load - ELO and Direct Integration Method comparison

In following figures, the comparison of ELO and Direct Integration Method is examined with a variable load, that represents the unbalanced load of washing machine. A sinusoidal signal with 1 Nm peak amplitude, 6 Hz frequency and 0.5 Nm offset is applied as a load torque. Also, at 0.5-0.8 s and 2-2.3 s time intervals a step load change of

2 Nm is applied as a test case. After 1.65 s feedforward compensation with load torque observer is activated. In feedforward compensation, since the real speed information of the simulation is used, it is highly effective to illustrate the effectiveness of the proposed compensation scheme. In figure 15 speed response of the system, speed PI has poor performance to keep tracking of the sinusoidally varied load profile. This resulted in exact sinusoidal fluctuation in the speed response. Motor speed is highly reduced in step change of load. After the compensation, control system is robust against the both sinusoidal and step changes. However it should be noted that after the feedforward compensation both observer schemes have even more ripples and ELO method performance is worse than the Direct Integration Method. In figure 16 torque response of the system, it can be seen that, motor torque is unable to track the load torque until the compensation. After the compensation, motor torque is coupled with the load torque in a reliable manner. Thereby, as it is examined in the figure 15, speed fluctuation is disappeared.

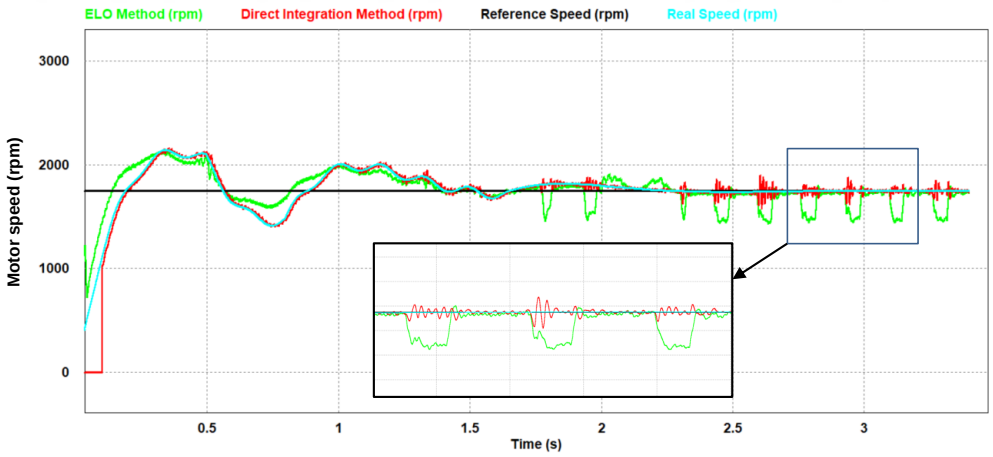

Figure 15: Speed response at variable load - ELO and direct integration method comparison

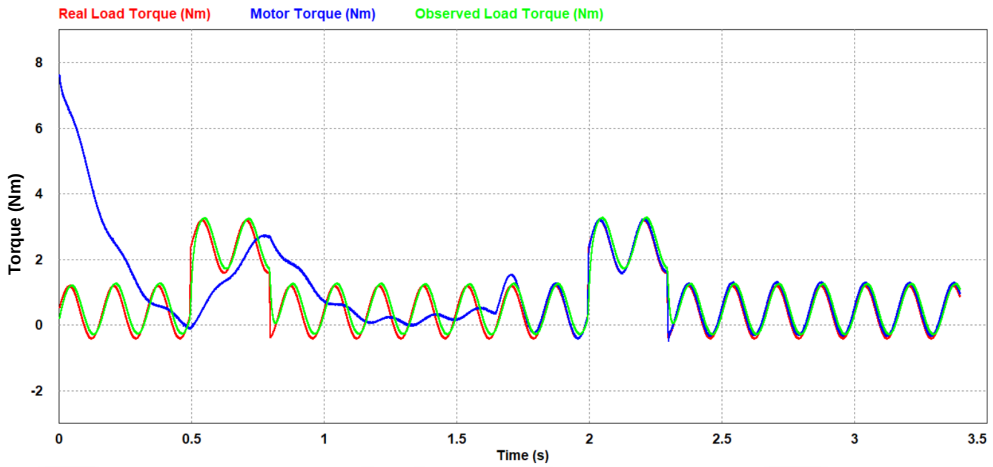

Figure 16: Torque response at variable load - ELO and direct integration method comparison

As a review of figure 13, 14, 15, 16 simulation studies, ELO and direct integration methods have nearly same performance in a constant load system. But when a variable load is used, ELO method has critical speed errors when compared with direct integration method. In any case, proposed compensation with load torque observer is effective to improve control system performance.

In next step, SMO and direct integration methods are compared in terms of speed response, usage in feedback control and usage in feedforward compensation. SMO method of the system is used in conjunction with super-twisting and PLL algorithms. Firstly, Direct Integration Method and SMO method speed responses are compared in figure 17 under the constant load profile of figure 14. It can be seen that, with SMO Method, speed fluctuation is highly reduced comparing with Direct Integration Method.

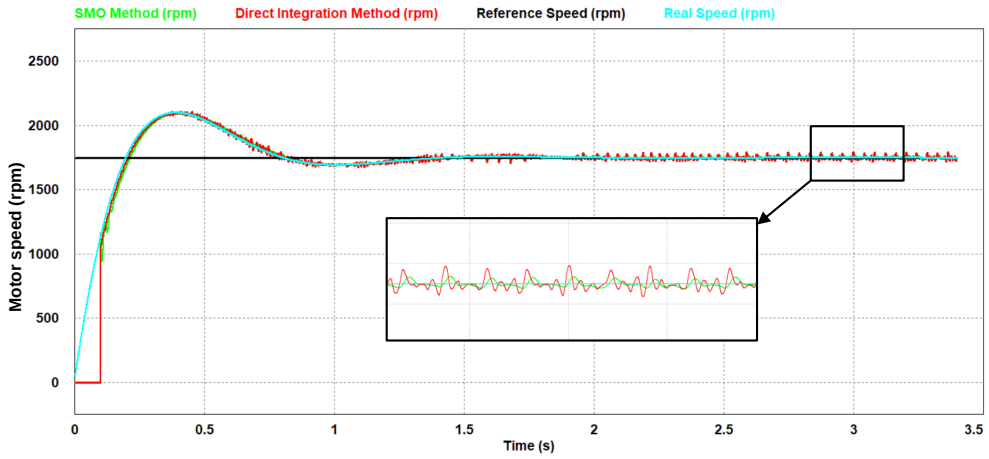

Figure 17: Speed response at constant load - SMO and direct integration method comparison

Secondly, system is tested under the real load profile of figure 16. Comparison of the motor speed response is given in figure 18. It can be seen that, as in constant load profile, speed fluctuation is highly reduced comparing with Direct Integration Method in washing machine load profile.

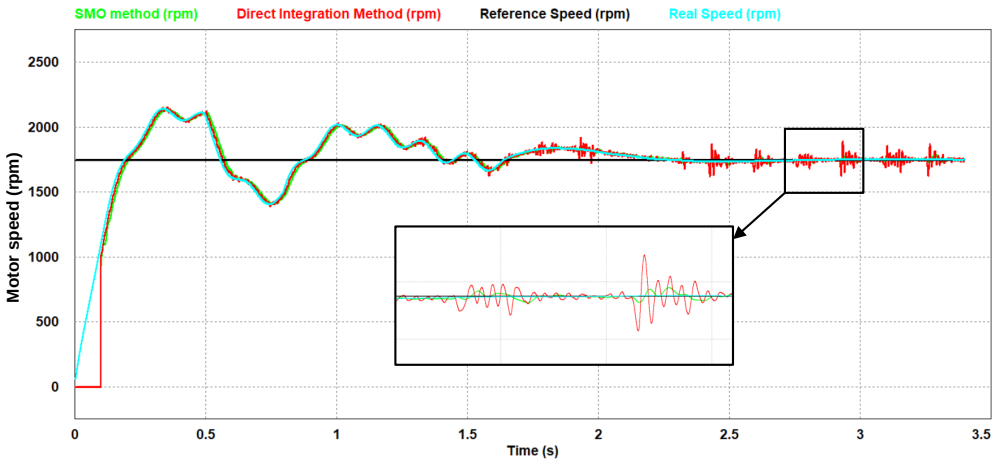

Figure 18: Speed response at variable load - SMO and direct integration method comparison

Next, for comparing the usage in feedback system of observed speeds, rotor position and motor information obtained from Direct Integration Method substituted with simulation's real parameters in control system. According to speed response in figure 19 there is not a remarkable change until the feedforward compensation, compared with system that uses the simulation parameters in figure 15. When the feedforward compensation activated with the load torque created by Direct Integration Method, motor control is almost lost. Then the system in the figure 19 is rearranged with substituting the rotor position and motor speed detection algorithm with SMO method. When the figure 20 is examined, it is not possible to see any remarkable difference with the system that uses the simulation parameters in figure 15 until the feedforward compensation. When the feedforward compensation is activated, effect of step load change in 2-2.3 s time interval is almost disappeared. Also it is possible to say that, speed fluctuation caused by sinusoidally varied load is decreased.

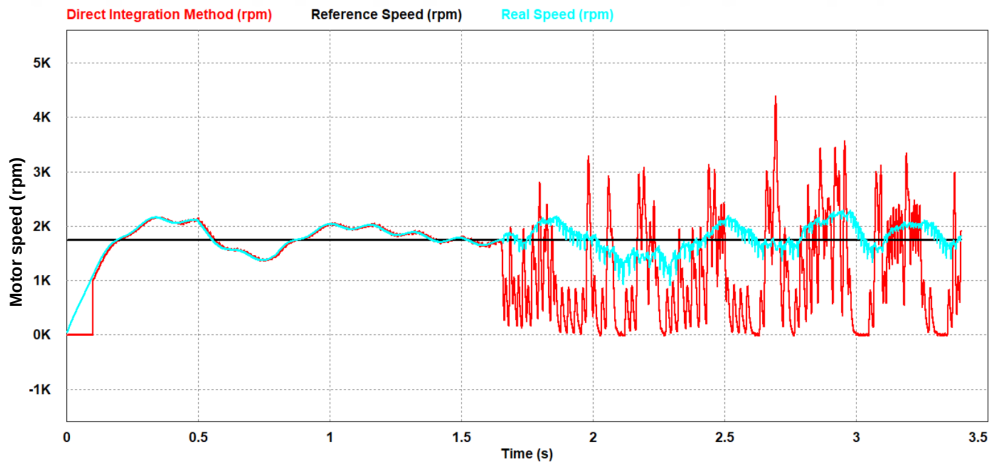

Figure 19: Speed response at variable load - feedback with Direct Integration Method

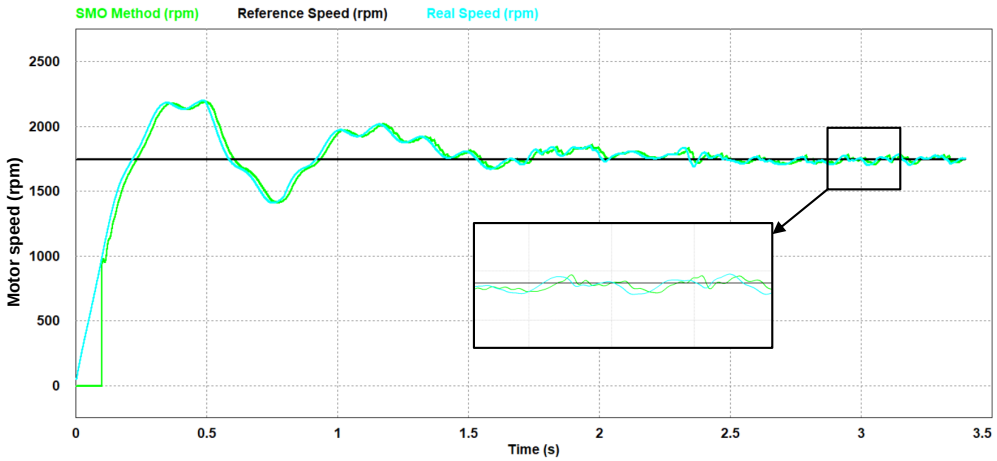

Figure 20: Speed response at variable load - feedback with SMO Method

As a review of figure 17, 18, 19, 20 simulation studies, SMO method has better performance under both constant and variable load of washing machine example comparing the direct integration and thereby ELO methods. For usage of SMO method in load torque observer, even it is not perfect as in the system that uses the simulation's parameters, load torque feedforward compensation is still effective to reduce speed fluctuation effects.

Lastly, at the following figures, load torque observers with PI control method and SMO method are compared. System is tested under variable load profile again and torque response is compared. Figure 21 represents the system which load torque observer is constructed with PI control and figure 22 is constructed with SMO load torque observer. Since SMO has the switching function as described in section 4.2, torque response contains fluctuations. Therefore even it has more phase lag compared with SMO, PI control is the better choice to be used as torque reference instead of more torque ripples.

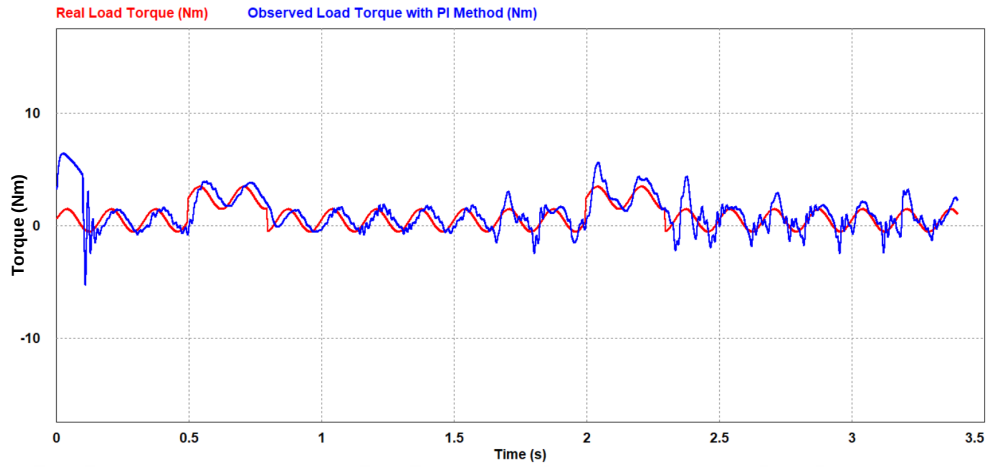

Figure 21: Torque response at variable load - load torque observer with PI Method

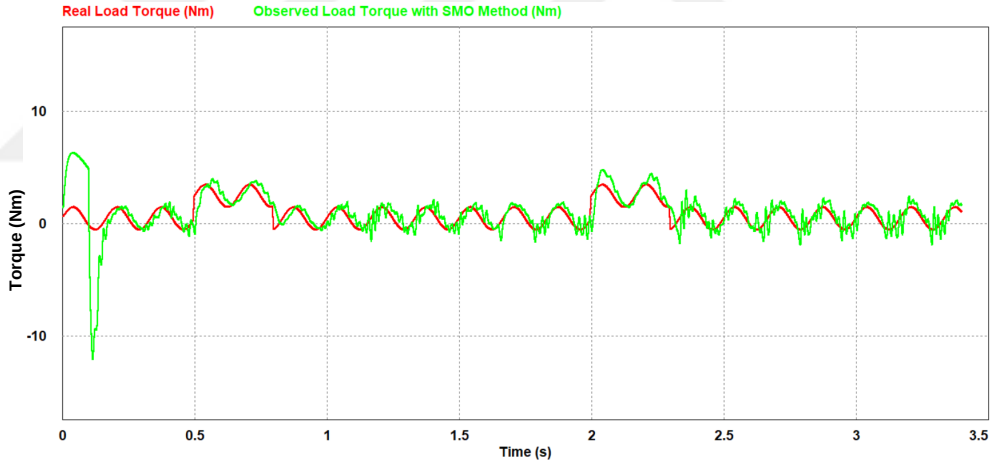

Figure 22: Torque response at variable load - load torque observer with SMO Method

In order to verify simulation results, experiments have been conducted in Vestel 9 kg capacity washing machine with the PMSM with following motor parameters.

Table 1: PMSM parameters

Characteristics	Units	Specification
Line resistance (phase to phase)	Ω	5.25
L_d / L_q at 50 Hz	mH	19.5/30
Line back-emf	V_{rms}	36
Polar couples	-	3

An inverter board "Vestel 20cmb05" is used which is included with Renesas RX63T family R5F563T4EDFL model microcontroller unit. In table 2 below, microcontroller and software specifications are given.

Table 2: Software Specifications

Item	Specification
Type of Motor	3 Phase PMSM
Motor Partname	LG Electronic WDB0300Y1M
Max MCU Frequecy	100 MHz
Multi Function Timer General PWM Timer	16 bit
3-Phase PWM Output Function	Yes
ADC	12 bit - 8 channel
Modulation Technique	Clamped PWM
Current Measurement	Three shunt current reading
Startup algorithms	Open loop startup Higher current than that rquired to win the load
Swithcing Frequency	16 kHz
Sampling Frequency	16 kHz

Software algorithm organization is referenced from Renesas YROTATE-IT-RX23T- Motor Control Kit. Flowchart of software organization and control interrupt routine can be found in figure 23 and 24.

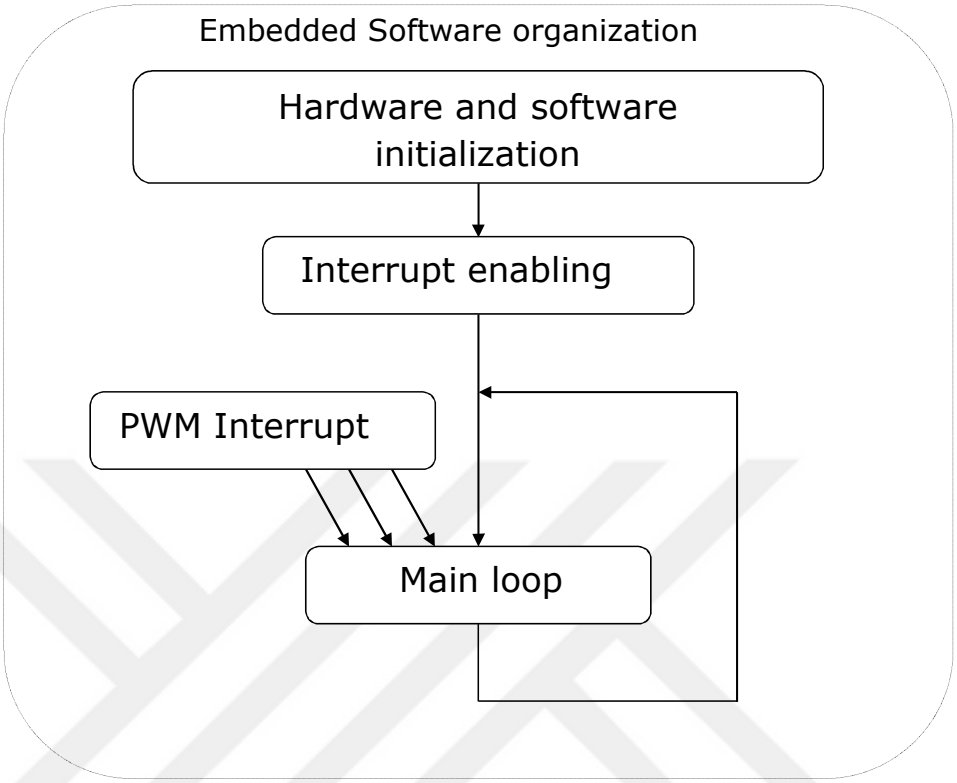

Figure 23: Software organization

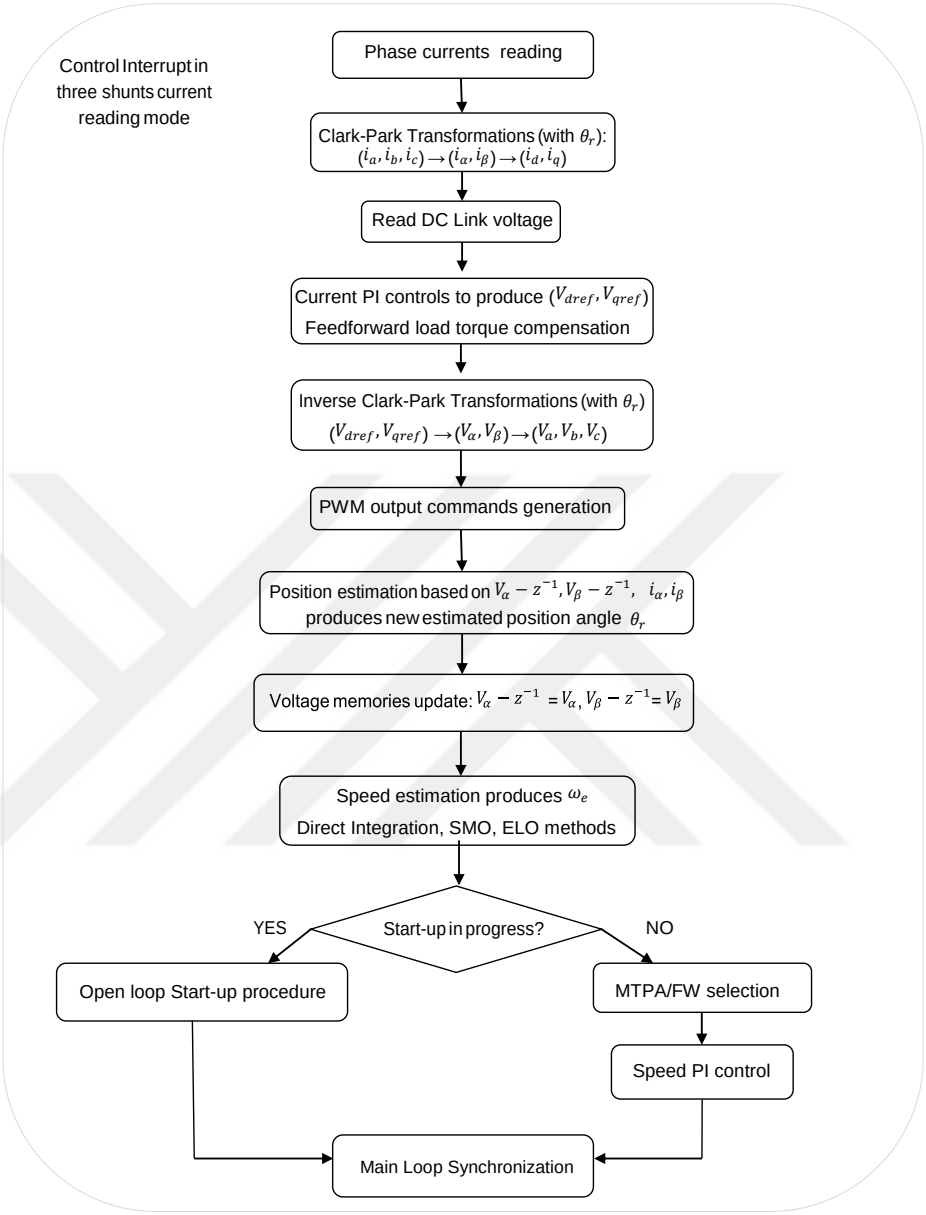

Figure 24: Control interrupt routine

5 kg unbalanced load is stacked in the drum of washing machine. Experimental setup can be seen in figure 25.

Figure 25: Experimental setup

Three different algorithms which are SMO scheme without load torque observer, Direct Integration Method without load torque observer and SMO Method with load torque observer are tested respectively. Motor speed reference is 1000 rpm and pulley ratio between drum and motor pulley is 11. Therefore washing machine rotates in 90.9 rpm. In this speed, laundries get stuck to drum walls because of the centrifugal force. In figure 26 below, system is driven by using the Direct Integration Method and the motor speed and motor torque values are demonstrated. Load torque compensation improvement is not included. As it's been demonstrated in simulations above, this method has more ripples in the speed feedback compared with SMO method. Therefore heavier filtering is required to be used in control and to have a smoother torque which is necessary to prevent mechanical damages. Therefore this situation limits the speed PI control performance and resulted in more fluctuations in motor speed and torque response. In this driving method, motor speed varies between 940 and 1060 rpm. Motor torque varies between -1.5 and 2 Nm.

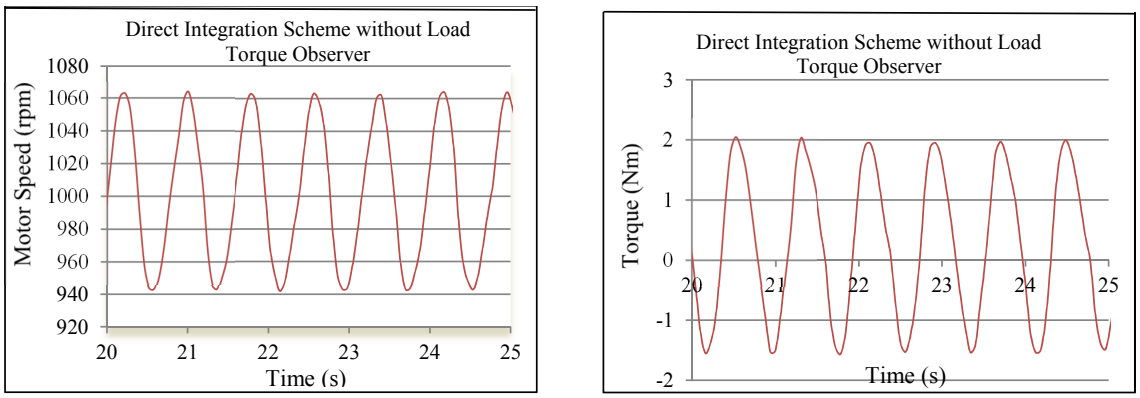

Figure 26: Motor speed and torque response - Direct Integration Method without load torque compensation

In figure 27 below system is driven by using the SMO Method and the motor speed and motor torque values are demonstrated. Load torque compensation improvement is not included. Since there are less fluctuations in motor speed and torque response filtering is not heavy as much as Direct Integration Method. This resulted with a better speed PI control performance. In this driving method, motor speed varies between 955 and 1050 rpm. Motor torque varies between -1.5 and 1.6 Nm.

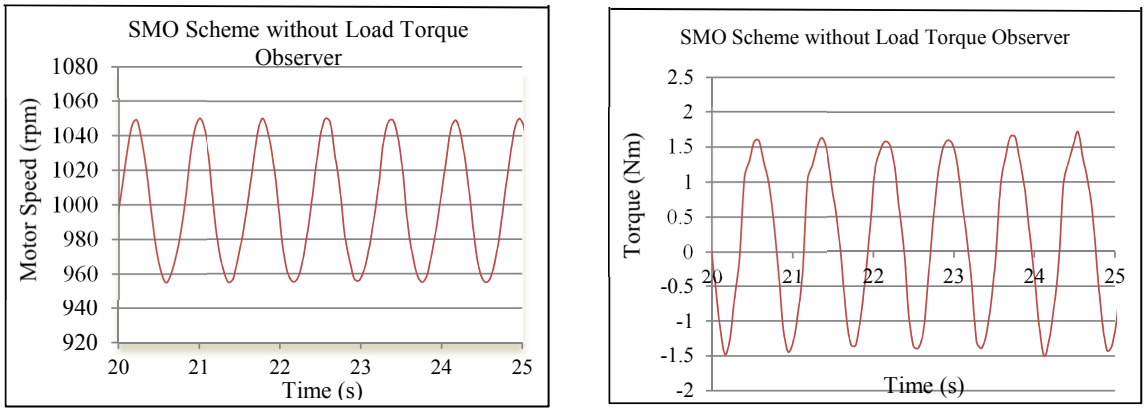

Figure 27: Motor speed and torque response - SMO Method without load torque compensation

Lastly in figure 28 below, system is driven by using the SMO Method and the motor speed and motor torque values are demonstrated. Load torque compensation improvement is included this time. Since system has the feedforward compensation in all time, there are less fluctuations in motor speed and torque response. This resulted with an improved speed PI control performance. In this driving method, motor speed varies between 980 and 1030 rpm. Motor torque varies between -1.3 and 1.5 Nm.

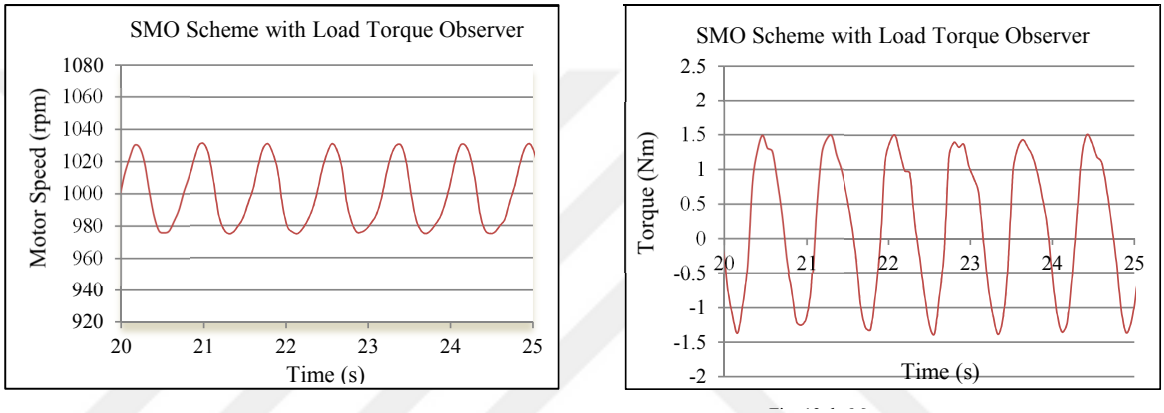

Figure 28: Motor speed and torque response - SMO Method with load torque compensation

As it is demonstrated in the figures above, with the help of SMO method and load torque feedforward compensation, speed fluctuation is now highly reduced and electromagnetic torque is now accurate. Since now motor speed fluctuation is decreased in figure 28, it is expected to have lower acoustical noise in driving system. In order to test this situation, acoustical noise test is performed. Two different method is operated in semi-anechoic test chamber and noise levels are compared in figure 29 below. While SMO method with feedforward compensation resulted in the average of 49.3 dB noise level, Direct Integration Method without load torque observer resulted around 50 dB noise level. It is a known fact that, 6-9 dB noise level differences cause to doubling or halving of loudness and 0.1-3 dB noise level differences cause to noticeable loudness

change. In washing machine application due to market requirement, lots of foams are used to get even 0.5 dB loudness decrease. When this situation considered, 0.7 dB noise level reduction with a driving method improvement can be considered as a remarkable change.

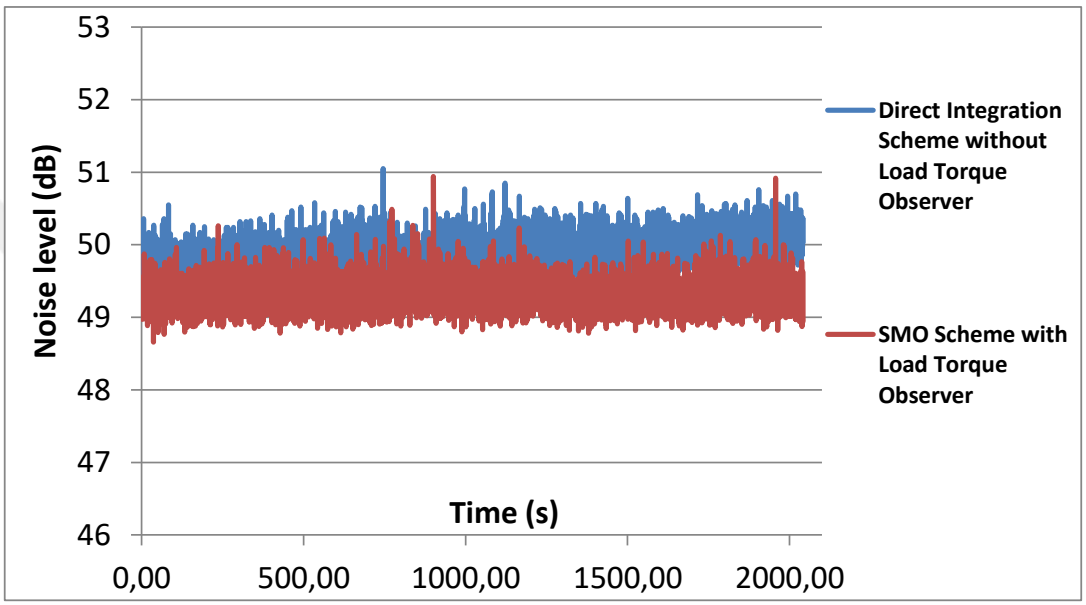

Figure 29: Acoustical noise level comparison - Direct Integration Method without load torque compensation and SMO Method with load torque compensation

Since the motor is now highly capable to track load torque and required motor torque is reduced in figure 28. It is expected to current in the motor is optimized. In order to test this, two different method is operated for 1,3 hours to check energy consumption values. As it can be seen from the table below energy consumption performance is improved which is crucial for washing machine marketing.

Table 3: Energy Consumption Values

Time (h)	Energy consumption (kWh) SMO Method with load torque observer	Energy consumption (kWh) Direct Integration Method without load torque observer
1.3	0.071	0.096

CHAPTER VII

CONCLUSION

A load torque compensation method for the PMSM of washing machine is presented in this paper. Three different speed and rotor position observer methods are studied. In order to improve the observer performances, a feedback signal method for Direct Integration Method, super-twisting method and PLL algorithms for SMO method are presented. These algorithms are compared in both feedback scheme and in load torque observer. Then the proposed feedforward compensation scheme is successfully implemented for the PMSM drive system of washing machine. Speed fluctuations and thereby acoustical noise is reduced with proposed feedforward method. Also, with the help of optimized motor torque, energy consumption is improved. Since there are better coupling between motor torque and load torque now, it is expected to have better durability of mechanical transmission parts in life time. The feasibility and effectiveness of the proposed technique is verified by simulations and experimental analysis.

Bibliography

[1] J. Wai and T. M. Jahns, "A new control technique for achieving wide constant power speed operation with an interior pm alternator machine," in *Conference Record of the 2001 IEEE Industry Applications Conference. 36th IAS Annual Meeting (Cat. No. 01CH37248)*, vol. 2, pp. 807–814, IEEE, 2001.

[2] L. Xheladini, A. Tap, T. Aşan, M. Yılmaz, and L. T. Ergene, "Permanent magnet synhronous motor and universal motor comparison for washing machine application," in *2017 11th IEEE International Conference on Compatibility, Power Electronics and Power Engineering (CPE-POWERENG)*, pp. 381–386, IEEE, 2017.

[3] A. Murray, M. Palma, and A. Husain, "Performance comparison of permanent magnet synchronous motors and controlled induction motors in washing machine applications using sensorless field oriented control," in *2008 IEEE Industry Applications Society Annual Meeting*, pp. 1–6, IEEE, 2008.

[4] A. Yorukoglu and E. Altug, "Determining the mass and angular position of the unbalanced load in horizontal washing machines," in *2009 IEEE/ASME International Conference on Advanced Intelligent Mechatronics*, pp. 118–123, IEEE, 2009.

[5] Y. Yuan, A. Buendia, R. Martin, and F. Ashrafzadeh, "Unbalanced load estimation algorithm using multiple mechanical measurements for horizontal washing machines," in *SENSORS, 2007 IEEE*, pp. 1303–1306, IEEE, 2007.

[6] L. Xuepeng, "Immune pi control on pmsm speed regulating system," in *2008 7th World Congress on Intelligent Control and Automation*, pp. 6891–6896, IEEE, 2008.

[7] R. Errouissi, A. Al-Durra, and S. Muyeen, "Experimental validation of a novel pi speed controller for ac motor drives with improved transient performances," *IEEE Transactions on Control Systems Technology*, vol. 26, no. 4, pp. 1414–1421, 2018.

[8] H. Zhang, H. Xu, C. Fang, and C. Xiong, "Design of a novel speed controller for direct-drive permanent magnet synchronous motor based on reduced-order load torque observer," in *2017 IEEE Transportation Electrification Conference and Expo, Asia-Pacific (ITEC Asia-Pacific)*, pp. 1–6, IEEE, 2017.

[9] A. M. El-Refaie, "Fractional-slot concentrated-windings synchronous permanent magnet machines: Opportunities and challenges," *IEEE Transactions on industrial Electronics*, vol. 57, no. 1, pp. 107–121, 2010.

[10] R. Krishnan, *Permanent magnet synchronous and brushless DC motor drives*. CRC press, 2009.

[11] N. Mohan, *Electric machines and drives: a first course*. No. 621.31042 M697e, Wiley,, 2012.

[12] P. C. Perera, *Sensorless control of permanent-magnet synchronous motor drives*. Institute of Energy Technology, Aalborg University, 2002.

[13] A. El-Sawy and E. Shehata, "Sensorless torque control of an ipmsm drive taking iron loss and saturation into account," *Journal of Engineering Sciences, Assiut University*, vol. 40, no. 2, pp. 533–555, 2012.

[14] A. Hassan, A. El-Sawy, Y. Mohamed, and E. Shehata, "Sensorless sliding mode torque control of an ipmsm drive based on active flux concept," *Alexandria Engineering Journal*, vol. 51, no. 1, pp. 1–9, 2012.

[15] Z. Zedong, L. Yongdong, M. Fadel, and X. Xi, "A rotor speed and load torque observer for pmsm based on extended kalman filter," in *2006 IEEE International Conference on Industrial Technology*, pp. 233–238, IEEE, 2006.

[16] H. Jiacai, L. Hongsheng, X. Qinghong, and L. Di, "Sensorless vector control of pmsm using sliding mode observer and fractional-order phase-locked loop," in *Proceedings of the 31st Chinese Control Conference*, pp. 4513–4518, IEEE, 2012.

[17] J. Davila, L. Fridman, and A. Levant, "Second-order sliding-mode observer for mechanical systems," *IEEE transactions on automatic control*, vol. 50, no. 11, pp. 1785–1789, 2005.

[18] P. Vas, *Sensorless vector and direct torque control*. Oxford Univ. Press, 1998.

[19] J. Solsona, M. I. Valla, and C. Muravchik, "Nonlinear control of a permanent magnet synchronous motor with disturbance torque estimation," *IEEE Transactions on Energy Conversion*, vol. 15, no. 2, pp. 163–168, 2000.

[20] C. Zhang, L. Jia, and J. He, "Load torque observer based sliding mode control method for permanent magnet synchronous motor," in *2013 25th Chinese Control and Decision Conference (CCDC)*, pp. 550–555, IEEE, 2013.

[21] Y. Liu, B. Zhou, and S. Fang, "Sliding mode control of pmsm based on a novel disturbance observer," in *2009 4th IEEE Conference on Industrial Electronics and Applications*, pp. 1990–1994, IEEE, 2009.

VITA

Koray Yoldaş is received the B.Sc. degree from Electrical and Electronics Engineering Department of Ege University, Izmir, Turkey, in 2015. He has been working at VESTEL Washing Machine Plant as R&D Engineer since 2015. His research interests are motor control systems, software design and power electronics.